Face-centred cubic to tetragonal transitions in In alloys under high pressure

2001 J. Phys.: Condens. Matter 13 7295

(http://iopscience.iop.org/0953-8984/13/33/310)

INSTITUTE OF PHYSICS PUBLISHING JOURNAL OF PHYSICS: CONDENSED MATTER

J. Phys.: Condens. Matter **13** (2001) 7295–7303 PII: S0953-8984(01)23901-0

Face-centred cubic to tetragonal transitions in In alloys under high pressure

O Degtyareva[1,2], V F Degtyareva[1], F Porsch[3] and W B Holzapfel[2]

[1] Institute of Solid State Physics, Russian Academy of Sciences, Chernogolovka, Moscow district, 142432 Russia
[2] FB 6 Physik, Universität-Paderborn, 33095 Paderborn, Germany
[3] Mineralogisch-Petrologisches Institute, Universität-Bonn, 53113 Bonn, Germany

Received 12 April 2001, in final form 11 June 2001
Published 2 August 2001
Online at stacks.iop.org/JPhysCM/13/7295

Abstract

The effect of pressure on the structural behaviour of In alloys with Cd, Sn and Pb has been studied with diamond anvil cells using synchrotron radiation. The face-centred cubic phase (fcc) of an In alloy with 6 at% Cd transforms under pressure into a face-centred tetragonal In-type phase, fct, with $c/a > 1$. The fcc phases of In alloys with 40 and 60 at% Pb transform under pressure to fct with $c/a < 1$. For the ambient pressure fct phase ($c/a < 1$) of an In alloy with 20 at% Sn the distortion increases with pressure. The stability of the tetragonal phases under pressure with respect to the cubic structure is discussed in terms of Brillouin-zone–Fermi-sphere interaction.

1. Introduction

The group III element In crystallizes in a body-centred tetragonal (bct) structure, tI2, space group $I4/mmm$. This bct structure represents a small distortion of the face-centred cubic, fcc, structure. Therefore, it is more convenient to describe it as face-centred tetragonal, fct, structure with an axial ratio $c/a = 1.0758$ [1]. A transition to fcc-In has not been observed neither at high temperature nor under high pressure. However, it has been reported that the axial ratio increases slightly with increasing pressure with a flat maximum around 25 GPa [2–4]. The lighter group III element Ga transforms under pressure to the fct In-type structure and at pressures above 100 GPa to fcc [5, 6], while Al, the lightest metal in this group, has fcc structure at ambient pressure and no phase transition has been observed up to 220 GPa [7]. The question of the stability of fcc and fct structures in the group III metals still attracts the attention of theorists [8, 9].

It is interesting to note that a change from fct to fcc occurs by the alloying of In with group II metals Cd or Hg [10]. The addition of these elements of lower valency decreases c/a of the fct structure resulting in an fcc structure at higher concentration. On the other hand, the addition of higher valency metals, like Sn or Pb, results in an increase of c/a and, at higher concentration,

c/a jumps from $c/a > 1$ to $c/a < 1$ [10]. This dependence of the axial ratio on the mean number of valence electrons, n, points to an electronic origin of the tetragonal distortion.

The interesting question is therefore, whether the fcc-In(Cd) alloy will be stable under high pressure. The same question arises with respect to the fcc phase existing at ambient pressure in the In–Pb alloys with In contents up to 60 at% [10, 11]. This paper presents the results of structural high-pressure studies on fcc phases in $In_{90}Cd_{10}$ and in In-Pb alloys ($In_{60}Pb_{40}$ and $In_{40}Pb_{60}$) and on the fct phase in $In_{80}Sn_{20}$.

2. Experimental

Alloys of In with Cd, Pb and Sn were prepared by melting appropriate amounts of the pure elements (5N purity). The alloys were characterized at ambient conditions by x-ray diffraction and were found to correspond to the known phase diagrams [11, 12]. Alloys of In with 40 and 60 at% Pb both have the fcc structure and $In_{80}Sn_{20}$ has the fct structure with $c/a < 1$, with lattice parameters close to the literature data [10]. For In with 10 at% Cd an fcc phase was observed with a small admixture of hcp-Cd. The lattice parameter of this fcc phase is $a = 469.7$ pm, close to the literature value of $a = 469.72$ pm for In–6 at% Cd [13].

High-pressure studies were performed with diamond anvil cells [14, 15] and energy dispersive diffraction using synchrotron radiation at DESY, HASYLAB [16, 17]. The ruby luminescence technique [18] was used for pressure measurements with the nonlinear ruby scale [19]. The alloy samples were loaded into the gasket hole with mineral oil as a pressure transmitting medium or without any transmitting medium because of the low shear modulus of In and In alloys. The high-pressure data for each of the four alloys were collected in two or three runs up to pressures of 30–37 GPa in steps of about 3 GPa on compression and about 5 GPa on decompression. Data in transition regions were collected in steps of about 1 GPa. Diffraction spectra were evaluated with the programs EDXPowd and XPOWDER [20].

3. Results

Phase transitions from fcc to fct structure were observed in In–Cd and In–Pb alloys with pressure increasing. Examples of diffraction patterns with fcc phase at ambient pressure and with fct phase at high pressure are shown for $In_{90}Cd_{10}$ in figure 1 and for $In_{60}Pb_{40}$ in figure 2.

The measured P–V data for the alloys are presented in figure 3 together with literature data for pure In [3, 21] and the fcc phase of Pb [22]. The ambient-pressure atomic volumes for the alloys are in agreement with Vegard's law. The variations of atomic volume with pressure are very similar to each other, differing only by a shift in atomic volume with alloy composition, according to the ambient pressure volume values. No significant volume changes are found at the fcc–fct transition. This is in agreement with the observed behavior at the fcc–fct transition in these alloys at ambient pressure with variation of alloy composition, where the respective volume change is less than 0.2% in these two-phase alloys [10].

The atomic volume data are fitted with an equation of state (EoS) using the first-order type AP1, discussed in detail previously [21–24]. Since the volume change at the fcc–fct transition is marginal, both phases have been fitted with one EoS, as shown by curves in figure 3. The atomic volume values V_0 are taken from ambient pressure measurements. The bulk modulus K_0 and its pressure derivative at ambient conditions K_0' for these alloys are close to the values for In [3, 21] and Pb [22], lying in the ranges 42–46 GPa and 4.5–6.0, respectively.

The variation of the axial ratio with pressure for the fct phases of these alloys is shown in figure 4. There are two kinds of tetragonal distortions of the fcc structure: one with $c/a > 1$ and one with $c/a < 1$.

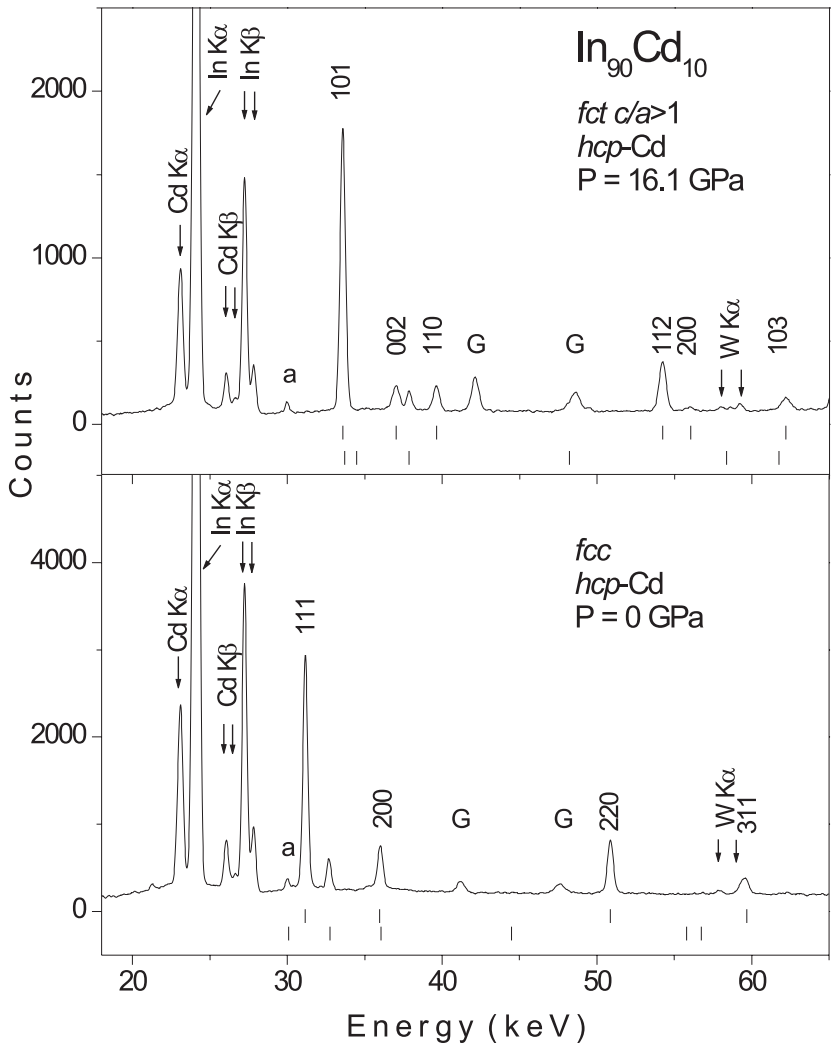

Figure 1. EDXD spectra for In–10 at% Cd collected with increasing pressure with $2\theta = 8.414^\circ$ ($Ed = 6307$ keV pm). Fluorescence peaks from In and Cd, marked by arrows, give evidence for the composition 90/10 in the In–Cd alloy. The pattern at $P = 0$ GPa contains an fcc phase with lattice parameter $a = 469.7(3)$ pm, and hcp-Cd with $a = 297.9$ pm, $c = 561.6$ pm. The pattern at $P = 16.1$ GPa shows an fct phase with lattice parameters $a = 426.6(2)$ pm, $c = 456.5(3)$ pm (face-centred setting), $c/a = 1.070$, and hcp-Cd with $a = 289.5(1)$ pm, and $c = 490.4(1)$ pm. The tick marks below each pattern show the peak positions for hcp-Cd (lower set) and for the fcc or fct phases (upper set). The Miller indices of fcc and fct reflections (body-centred setting) are given. Reflections from gasket material are denoted by G, 'a' denotes an electronic artefact observed with this set up at low count rates. The fluorescence peaks from W originating from the collimating system are marked by arrows.

3.1. In–Cd

The diffraction pattern of $In_{90}Cd_{10}$ at ambient pressure corresponds to an fcc phase with a small admixture of hcp–Cd (figure 1). When the pressure is increased to 1.4 GPa, a transition from fcc to fct takes place with a discontinuous change of the axial ratio from $c/a = 1$ to

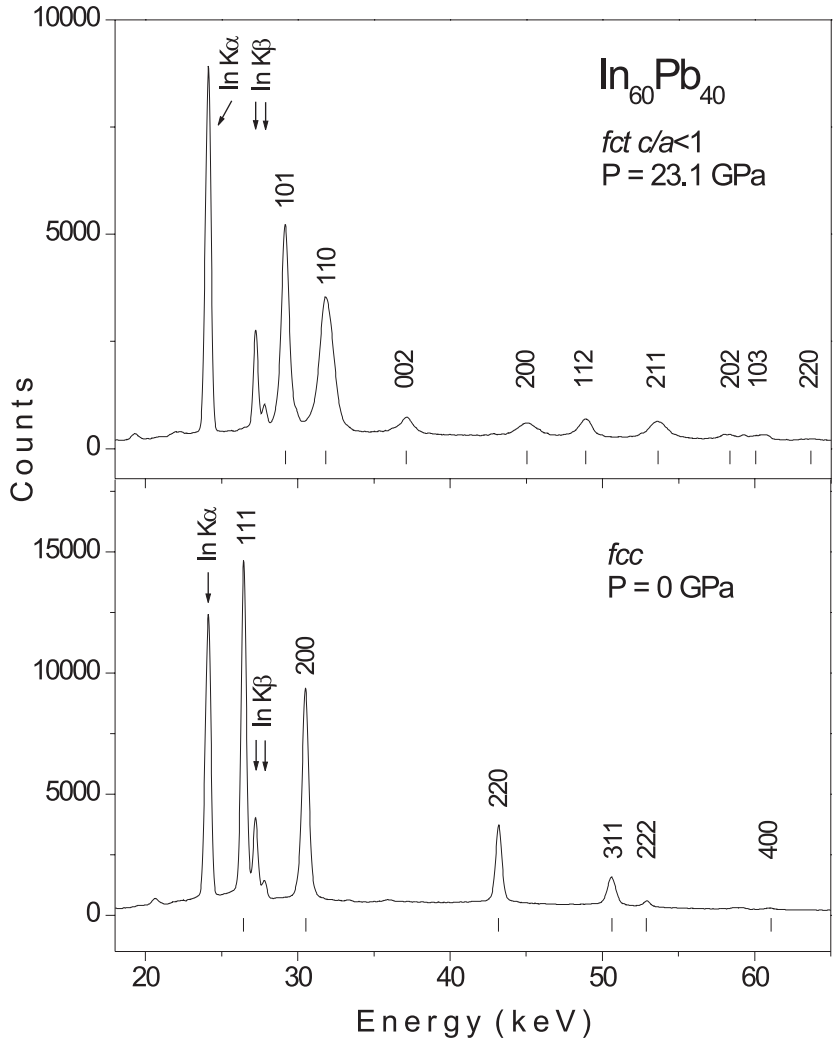

Figure 2. EDXD spectra of $In_{60}Pb_{40}$ collected with $2\theta = 9.634^{\circ}$ ($Ed = 7383$ keV pm) with increasing pressure. Fluorescence peaks from In are marked by arrows. The ambient pressure fcc phase has the lattice parameter $a = 483.5(2)$ pm. Lattice parameters for the tetragonal phase at 23.1 GPa are $a = 463.9(2)$ pm, $c = 397.8(4)$ pm (face-centred setting), c/a = 0.858. The tick marks below each pattern show the calculated peak positions. Miller indices for the reflections of fcc and fct (body-centred setting) are given.

$c/a = 1.037$ with $a = 460.2(2)$ pm and $c = 470.0(4)$ pm in the fct setting. This fct phase remains stable up to 30.4 GPa—the highest pressure reached in this study. The axial ratio of fct increases with pressure up to 1.074, as shown in figure 4, similarly to pure In [3, 21] but with a somewhat lower c/a.

There is no indication of a change of the composition of the alloy at the fcc–fct transition, and the diffraction peaks of hcp-Cd persist across the transition. The possible volume discontinuity at the fcc–fct transition is smaller than the resolution of the present experiments ($\Delta V/V \leqslant 0.5\%$).

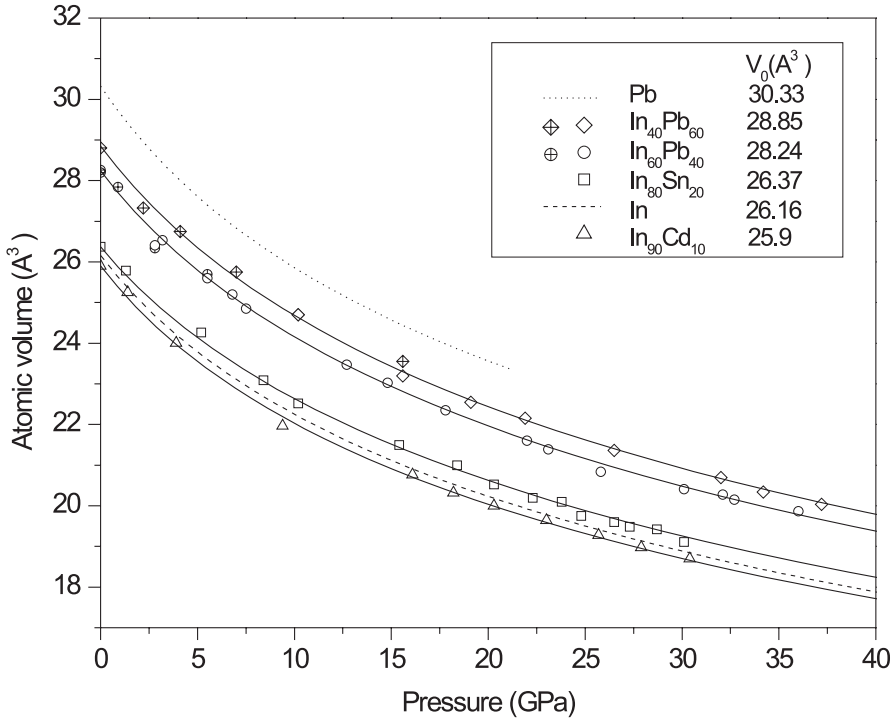

Figure 3. Pressure dependence of the atomic volume for the fcc and fct phases of In alloys with Pb, Sn and Cd. The open and crossed symbols denote fct and fcc phases, respectively. The full curves represent fits using a first-order equation of state with the parameter values discussed in the text. For comparison the P–V data for pure In [3, 21] and also for the fcc phase of Pb [22] are shown by the broken and dotted curves, respectively.

The reverse fct–fcc transformation was observed on decreasing pressure with a remarkable hysteresis in the variation of the axial ratio. At ambient pressure the fcc phase is recovered. The pressure–volume relation for the fct phase of this In–Cd alloy is very similar to pure In [3, 21] with a slightly smaller volumes, as shown in figure 3.

3.2. In–Pb

In the In–Pb system three different alloys with compositions 40, 60 and 80 at% Pb were studied. All these alloys exhibit at ambient pressure an fcc phase with lattice parameters 483.4(1), 486.8(1) and 491.4(1) pm, respectively. Corresponding to the Pb content the lattice parameter increases (Vegard's law) towards to the value 495.04 pm, the lattice parameter of pure Pb [10].

The alloys $In_{60}Pb_{40}$ and $In_{40}Pb_{60}$ show similar behaviour under pressure. Both alloys transform under pressure from fcc to fct with $c/a < 1$. The diffraction patterns of $In_{60}Pb_{40}$ in its fcc phase at ambient pressure and its high-pressure fct phase are shown in figure 2. In $In_{60}Pb_{40}$ the transformation from fcc to fct occurs at approximately 2–3 GPa, whereas in $In_{40}Pb_{60}$ it occurs at about 10 GPa. The fcc–fct transition shows a region of indifference of about 5 GPa in pressure. At the fcc–fct transition the axial ratio changes discontinuously from 1 to 0.94 in $In_{60}Pb_{40}$ and to 0.915 in $In_{40}Pb_{60}$. When the pressure is increased, the axial ratio decreases further (figure 4). The fcc–fct transformation is reversible in both alloys with some hysteresis and the fcc phase is recovered on decompression.

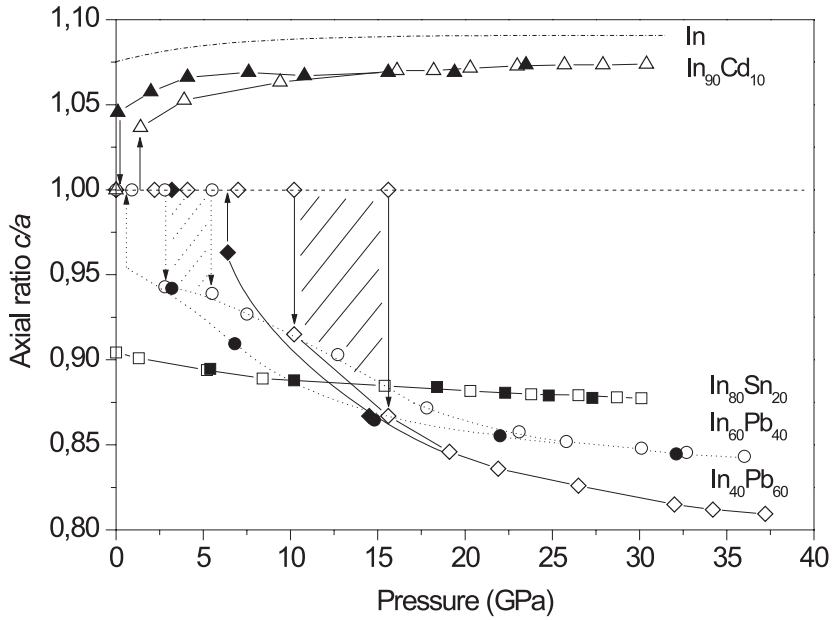

Figure 4. Variations of the axial ratio c/a with pressure for the alloys of In with Cd, Sn and Pb with increasing and decreasing pressure marked by open and closed symbols, respectively. The axial ratio for the tetragonal phase is given in the fct setting to illustrate the relation to fcc ($c/a = 1$). For comparison the c/a data of pure In [3, 21] are shown by the chain curve. The arrows mark discontinuous changes of axial ratios at the fcc–fct transition. Dashed areas indicate the two-phase regions in the In–Pb and In–Sn alloys. The full and dotted curves connecting the experimental data are guides to the eye.

The behaviour of the Pb-rich alloy $In_{20}Pb_{80}$ is different. At 17 GPa it transforms from fcc to hcp. The fcc–hcp transition is reversible with a hysteresis of about 5 GPa. Pure Pb shows the same transition but at a lower pressure of 13 GPa [25]. The lattice parameters of hcp $In_{20}Pb_{80}$ at 35.1 GPa are $a = 308.1(1)$ pm, $c = 505.4(3)$ pm, and $c/a = 1.640$, compared with Pb at 36.4 GPa with $a = 311.3(2)$ pm, $c = 510.5(6)$ pm, and $c/a = 1.640$ [22].

3.3. In–Sn

The In alloy with 20 at% Sn with its ambient pressure fct phase has been studied up to 30 GPa. The fct structure was found to be stable up to the highest pressure reached, whereas a degree of tetragonal distortion increases. The axial ratio decreases from the ambient pressure value $c/a = 0.904$ down to 0.877 at 30 GPa (figure 4). On decompression, c/a increases reversibly. The change in c/a for this alloy is much weaker than the decrease of c/a in the $In_{60}Pb_{40}$ and $In_{40}Pb_{60}$ alloys. There is a correlation between the observed degree of distortion (c/a) and the valence electron concentration for these three alloys, which is 3.2, 3.4 and 3.6 electron/atom for $In_{80}Sn_{20}$, $In_{60}Pb_{40}$ and $In_{40}Pb_{60}$, respectively. The larger the electron concentration, the lower the c/a value, if compared at one pressure.

4. Discussion

High-pressure studies on fcc alloys of In with Cd and Pb show that the fcc phase is unstable under pressure and transforms to an fct phase either with $c/a > 1$ or with $c/a < 1$. This is

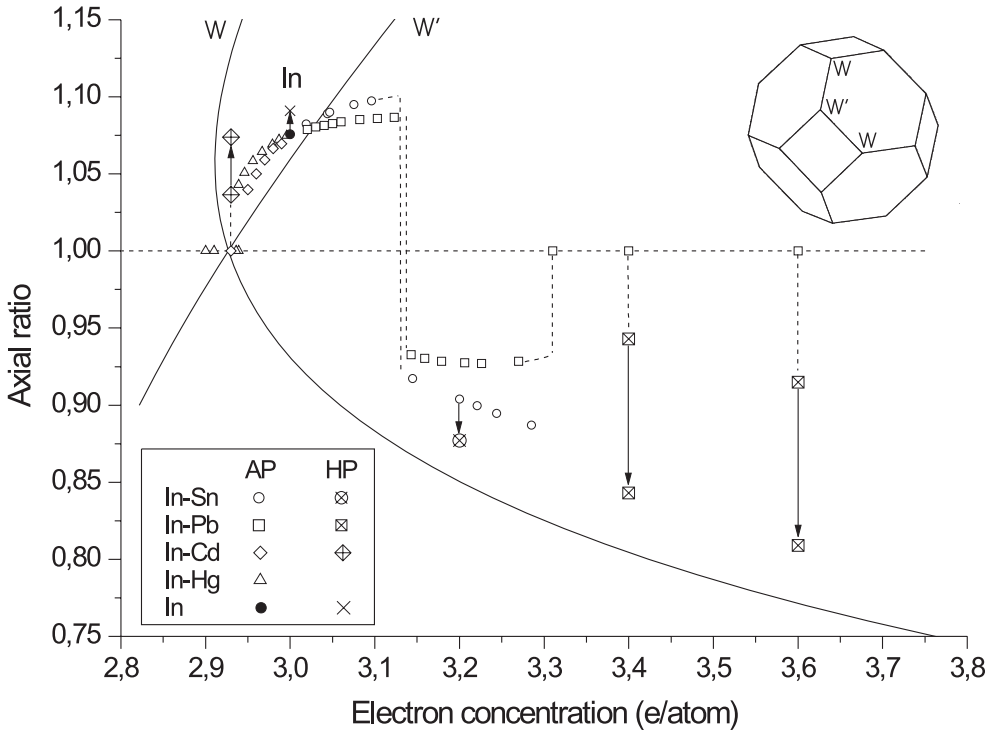

Figure 5. Axial ratio against electron concentrations for fct phases in In-alloys at ambient pressure (open symbols) from [10] and at high pressure (crossed symbols) from the present work. The full circle and cross correspond to the data on In at normal and high pressure (23 GPa [3,21]). The arrows show the change of c/a under pressure from the value just at the fcc–fct transition to the value at the highest pressure reached in this study. The full curves represent the calculated distortion (c/a against n) when the Brillouin zone corners of type W and W′ touch the free electron Fermi sphere determined by n [26]. The Brillouin zone of the fcc structure is shown in the upper right corner.

consistent with the observation of two different types of fct phases with $c/a > 1$ and with $c/a < 1$ in In alloys at ambient pressure (figure 5). The parameter controlling the axial ratio is the mean electron concentration, n. At the electron concentration $n = 3.12$–3.15 the axial ratio switches from $c/a > 1$ to $c/a < 1$.

The fcc–fct distortion can be understood if one considers two contributions to the crystal energy: (1) the electrostatic Ewald term; and (2) the electronic band-energy contribution due to Fermi-sphere (FS)–Brillouin-zone (BZ) interaction. The electrostatic energy calculated for a common tetragonal structure along the deformation from fcc to bcc has two minima [8] corresponding to $c/a = 1$ (fcc) and $c/a = 1/\sqrt{2}$ (bcc) indicating that this term favours high-symmetry cubic structures and the tetragonal distortion is caused by other terms.

With respect to the electronic band-energy contribution In and the neighbouring metals (Cd, Sn and Pb) can be regarded as sp-bonded nearly-free electron metals with an almost spherical Fermi surface. In the case of trivalent metals the first Brillouin zone of the fcc lattice lies inside the FS. However, the corners of the BZ of W-type are close to the FS. A small lattice distortion can shift these corners to the Fermi surface. This will lower the electronic band energy and stabilize the distortion. Two different kinds of tetragonal distortion are possible, shifting either the corner W or W′ to the Fermi surface. Figure 5 shows the calculated variation

of the axial ratio with electron concentration for these two kinds of distortion [26]. For $n = 2.94$ all W and W′-type corners are in contact with the Fermi surface resulting in a symmetric fcc structure. From this point of view, the formation of the fcc phase in In–Cd and In–Hg alloys in a narrow concentration range around 6 at% Cd or Hg (e.g. at $n = 2.94$) can be understood.

According to this model, one can consider the stabilizing of either fcc or fct as a result of the balance between electrostatic and electronic band-energy terms. The latter contribution to the crystal energy appears to become more significant under pressure, stabilizing the tetragonal distortion.

For the In–Cd alloy with electron concentration n < 3.12 the axial ratio follows the upper branch of c/a against n, as shown in figure 5. The same reasoning leads to the increase of c/a with pressure for the tetragonal structure of pure In.

For the In–Pb alloys with electron concentrations $n > 3.12$ the tetragonal distortion follows the lower branch with $c/a < 1$. A remarkable observation is the trend of increasing distortion (by the lowering of c/a) with increasing pressure or increasing electron concentration. The high-pressure fct phases with $c/a < 1$ correspond to the fct phases observed in this system at normal pressure in the range from ∼15 to ∼30 at% Pb. Thus pressure causes the expansion of the fct region towards Pb. It should be pointed out that pure Pb has no fct phase but transforms to hcp at 13 GPa. A similar expansion of the fct region was derived in the In–Tl system from measurements of superconductiviy [27], indicating that high pressure stabilizes tetragonal distortions with respect to the cubic structures in In-alloys for a wide range of different solutes (Cd, Sn, Pb and Tl). It is known that heavy elements like Pb are characterized by relativistic effects (see, e.g. [28]), which should be considered by quantitative calculations. The nearly-free-electron model provides a qualitative explanation for the stabilization of tetragonally distorted face-centred structure and the c/a dependence on electron concentration.

5. Conclusion

Experimental results on c/a for fct phases obtained under pressure in In alloys with Cd or with Sn and Pb display a trend for c/a to approach the plot calculated for the touching of the Brillouin zone corners to the Fermi sphere. These observations support this model at least qualitatively, explaining the instability of the fcc structure with respect to tetragonal distortions in In and In alloys and the trends in the variation of c/a with electron concentration and with pressure.

Acknowledgments

The authors wish to thank W Sievers and W Bröckling for technical assistance. The financial support by the Russian Foundation for Basic Research under the grant number 01-02-97030 and by the Deutsche Forschungsgemeinschaft under grant number 436 RUS 17/74/99 is gratefully acknowledged.

References

[1] Villars P and Calvert L D 1985 *Pearson's Handbook of Crystallographic Data for Intermetallic Phases* (Metals Park, OH: American Society for Metals)

[2] Vereshchagin L F, Kabalkina C C and Troitskaja Z V 1964 *Dokl. Acad. Nauk SSSR* **158** 1061 (Engl. Transl. 1965 *Sov. Phys.–Dokl.* **9** 894)

[3] Takemura K 1991 *Phys. Rev.* B **44** 545

[4] Schulte O, Nikolaenko A and Holzapfel W B 1991 *High Press. Res.* **6** 169
[5] Schulte O and Holzapfel W B 1997 *Phys. Rev.* B **55** 8122
[6] Takemura K, Kobayashi K and Arai M 1998 *Phys. Rev.* B **58** 2482
[7] Greene R G, Luo H and Ruoff A L 1994 *Phys. Rev. Lett.* **73** 2075
[8] Heine V and Weaire D 1970 *Solid State Physics* vol 24 (New York: Academic) p 459
[9] Simak S I, Haeussermann U, Ahuja R, Lidin S and Johansson B 2000 *Phys. Rev. Lett.* **85** 142
[10] Pearson W B 1964 *A Handbook of Lattice Spacings and Structures of Metals and Alloys* (Oxford: Pergamon)
Pearson W B 1967 *A Handbook of Lattice Spacings and Structures of Metals and Alloys* vol 2 (Oxford: Pergamon)
[11] Hansen M and Anderko K 1958 *Constitution of Binary Alloys* (New York: McGraw Hill) (reprinted 1989 New York: Genium)
[12] Massalsky T B 1986 *Binary Alloy Phase Diagrams, American Society for Metals* (Metals Park, OH: American Society for Metals)
[13] Straumanis M E, Rao P B and James W J 1971 *Z. Metal.* **62** 493
[14] Syassen K and Holzapfel W B 1975 *Europhys. Conf. Abstr.* **1A** 75
[15] Holzapfel W B 1978 *High Pressure Chemistry* ed H Kelm (Dordrecht: Reidel) pp 177–97
[16] Grosshans W A, Düsing E F and Holzapfel W B 1984 *High Temp.–High Pressures* **16** 539
[17] Otto J W 1997 *Nucl. Instrum. Methods Phys. Res.* A **384** 552
[18] Forman R A, Piermarini G J, Barnett J D and Block S 1972 *Science* **176** 284
[19] Mao H K, Bell P M, Shaner J W and Steinberg D J 1978 *J. Appl. Phys.* **49** 3276
[20] For the programs for the evaluation of EDXD spectra see Porsch F 1995 *EDXPowder and XPOWDER* (Paderborn, Germany: RTI)
[21] Schulte O and Holzapfel W B 1993 *Phys. Rev.* B **48** 767
[22] Schulte O and Holzapfel W B 1995 *Phys. Rev.* B **52** 12 636
[23] Holzapfel W B 1998 *High Press. Res.* **16** 81
[24] Holzapel W B 2001 *Rev. High Pressure Sci. Technol.* **11** 55
[25] Takahashi K, Mao H K and Basset W A 1969 *Science* **165** 1352
[26] Svechkarev I V 1964 *Zh. Eksp. Teor. Fiz.* **47** 961 (See Engl. Transl. 1965 *Sov. Phys.–JETP* **20** 643)
[27] Smith T F and Finlayson T R 1994 *Phys. Rev.* B **49** 12 559
[28] Christensen N E, Satpathy S and Pawlowska Z 1986 *Phys. Rev.* B **34** 5977